Izv. Vyssh. Uchebn. Zaved. Khim. Khim. Tekhnol. 2016. V. 59. N 10

DOI: 10.6060/tcct.20165910.5431

Для цитирования:
Ефремов А.М., Kwon K.-H., Шабадарова Д.А. Сравнительное исследование параметров и состава плазмы в смесях CF_4, Cl_2 и HBr + Ar. *Изв. вузов. Химия и хим. технология*. 2016. Т. 59. Вып. 10. С. 11−18.
For citation:
Efremov A.M., Kwon K.-H., Shabadarova D.A. Comparative study of plasma parameters and compositions in CF_4, Cl_2 and HBr + Ar gas mixtures.. *Izv. Vyssh. Uchebn. Zaved. Khim. Khim. Tekhnol*. 2016. V. 59. N 10. P. 11−18.

УДК: 537.525

А.М. Ефремов, K.-H. Kwon, Д.А. Шабадарова

Александр Михайлович Ефремов (🖂), Дария Александровна Шабадарова

Кафедра технологии приборов и материалов электронной техники, Ивановский государственный химико-технологический университет, Шереметевский пр., 7, Иваново, 153000, Российская Федерация
E-mail: efremov@isuct.ru (🖂)

K.-H. Kwon

Лаборатория применения плазмы, Департамент разработки средств и методов контроля, Университет Корея, 208 Сеочанг-Донг, Чочивон, 339-800, Республика Корея

СРАВНИТЕЛЬНОЕ ИССЛЕДОВАНИЕ ПАРАМЕТРОВ И СОСТАВА ПЛАЗМЫ В СМЕСЯХ CF_4, Cl_2 И HBr + Ar

В данной работе обсуждаются электрофизические параметры и химия плазмы в системах CF_4 + Ar, Cl_2 + Ar и HBr + Ar при одинаковых условиях возбуждения разряда. Исследования проводились методами диагностики плазмы зондами Лангмюра и моделирования плазмы в условиях планарного индукционного плазмохимического реактора при постоянном давлении газа (10 мТор), вкладываемой мощности (800 Вт) и мощности смещения (300 Вт), но при варьируемой (0-80%) доле Ar в плазмообразующей смеси. Основное внимание уделялось параметрам, определяющим стационарные концентрации активных частиц плазмы (температура электронов, концентрация электронов, константы скоростей реакций под действием электронного удара) и кинетику гетерогенных ионно-стимулированных химических реакций (потоки атомов галогенов, энергия ионной бомбардировки, поток энергии ионов).

Ключевые слова: CF_4, Cl_2, HBr, плазма, константа скорости, скорость реакции, поток атомов галогенов, поток энергии ионов

UDC: 537.525

A.M. Efremov, K.-H. Kwon, D.A. Shabadarova

Alexander M. Efremov (✉), Dariya A. Shabadarova

Department of Electronic Devices and Materials Technology, Ivanovo State University of Chemistry and Technology, Sheremetevskiy ave., 7, Ivanovo, 153000, Russia
E-mail: efremov@isuct.ru (✉)

Kwang H. Kwon

Plasma Application Lab., Dept. of Instrumentation and Control Engineering, Korea University, 208 Seochang-Dong, Chochiwon, 339-800, Korea

COMPARATIVE STUDY OF PLASMA PARAMETERS AND COMPOSITIONS IN CF_4, Cl_2 AND HBr + Ar GAS MIXTURES

This work discusses the plasma characteristics and chemistry in CF_4 + Ar, Cl_2 + Ar and HBr + Ar gas systems under one and the same operating condition. The investigation was carried out using the combination of plasma diagnostics by Langmuir probes and 0-dimensional plasma modeling in the planar inductively coupled plasma reactor at constant gas pressure (10 mTorr), input power (800 W) and bias power (300 W), but with variable (0–80%) Ar fraction in a feed gas.The main attention was attracted to the parameters influencing the steady-state densities of plasma active species (electron temperature, electron density, electron-impact rate coefficients) and the kinetics of ion-assisted chemical reaction (fluxes of halogen atoms, ion bombardment energy, ion energy flux).

Keywords: CF_4, Cl_2, HBr, plasma, rate coefficient, reaction rate, halogen atom flux, ion energy flux

INTRODUCTION

Low-temperature plasma in halogenated gases has found wide application in micro- and nano-electronics for the dry etching of semiconductor wafers and functional layers when the wet technologies do not meet the requirements on the purity, resolution, and reproducibility of the process [1-3]. Since the most of dry etching processes are driven by the halogen atoms formed in plasma due to the dissociation of the feed gas molecules [4-6], many types of fluorine-, chlorine and bromine-containing gases, including CF_4, Cl_2 and HBr, have been involved in practical use.

Until now, there were enough experimental and modeling works for CF_4^- [7-12], Cl_2 [13-19] and HBr^- [20-22] based plasmas. These works contain the well-adjusted kinetic schemes for plasma chemical reactions as well as provide the clear understanding of the main kinetic effects determining the steady-state plasma parameters in each gas system. However, since one and the same material can be etched in all three (or, at least, in two) gas chemistries, the key issue is to know and to understand the difference in plasma parameters determining the kinetics of ion-assisted chemical reaction. Unfortunately, the existing works cannot provide the direct comparison for F^-, Cl- and Br-based gas chemistries because the corresponding results were obtained under the different sets process conditions and/or in the reactors with different geometries. Therefore, the comparative study of F-, Cl- and Br-based gas chemistries is still an important task to be solved for the better optimization of dry etching technologies.

In this work, we performed the model-based comparative study of CF_4 + Ar, Cl_2 + Ar and HBr + Ar plasmas under one and the same operating condition. In each case, we selected the simplest halogen-containing gas which can serve as the source of F, Cl or Br atoms. The main goal was to figure out the dif-

ferences in plasma parameters determining the kinetics of the heterogeneous ion-assisted chemical reaction as well as to understand the nature of these differences through the formation-decay kinetics of plasma active species.

EXPERIMENTAL AND MODELING DETAILS

Plasma diagnostics experiments were performed in a planar inductively coupled plasma (ICP) reactor described in our previous works [19–22]. The experiments were performed at a fixed total gas flow rate (q = 40 sccm), gas pressure (p = 10 mTorr), input power (W = 800 W) and bias power (W_{dc} = 300 W). The CF_4/Ar, Cl_2/Ar and HBr/Ar mixing ratios were set in the range of 0-80% Ar by adjusting the partial gas flow rates within q = const. Accordingly, the fraction of Ar in a feed gas was $y_{Ar} = (q_{Ar}/q)$.

Plasma parameters were measured by double Langmuir probe (DLP2000, Plasmart Inc., Korea). The treatment of $I – V$ curves aimed at obtaining electron temperature (T_e) and ion saturated current density (j_+) was carried out using the software supplied by the equipment manufacturer. The calculations were based on the Johnson & Malter's double probes theory [23] with the one-Maxwellian approximation for the electron energy distribution function (EEDF). The total positive ion density (n_+) was extracted from the measured j_+ using the Allen-Boyd-Reynolds (ABR) approximation [24].

In order to obtain the electron density and the densities of neutral species, we developed a simplified zero-dimensional kinetic model [25-27] with using the l data of T_e and n_+ as input parameters. The sets of chemical reactions were taken from our previous works [12, 19, 20]. The model used following assumptions: 1) The EEDF is close to Maxwellian one. This allows one to obtain the rate coefficients for the electron-impact processes as functions of T_e in a form of $k = AT_e^B\exp(-C/T_e)$; 2) The heterogeneous chemistry of atoms and radical in all three gas systems can be described in terms of the conventional first-order recombination kinetics [6, 25–27]; and 3) The temperature of the neutral ground-state species (T_{gas}) is independent on the feed gas composition. Since the experimental data on gas temperature were not available in this study, we took T_{gas} = 600 K as the typical value for the ICP etching reactors with similar geometry under the close range of experimental conditions [19-22].

The electron density (n_e) was calculated using the simultaneous solution of the steady-state chemical kinetic equation for negative ions $\nu_{da}n_e \approx \approx k_{ii}n_+n_-$ and the quasi-neutrality equation $n_+ = n_e + n_-$. These allow one to obtain

$$n_e \approx \frac{k_{ii}n_+^{\ 2}}{\nu_{da} + k_{ii}n_+}$$

where ν_{da} is the total frequency of dissociative attachment, n_- is the density of negative ions, and k_{ii} is the rate coefficient for ion-ion recombination. The steady-state densities for neutral ground-state plasma components were obtained from the system of chemical kinetics equations in the general form of $R_F – R_D = =(k_S + 1/\tau_R)n$, where R_F and R_D are the volume-averaged formation and decay rates in bulk plasma for a given type of species, n is their density, k_S is the first-order heterogeneous decay rate coefficient, and $\tau_R = \pi r^2 lp/q$ is the residence time.

The adequacy of the given modeling algorithm, kinetic schemes and general approaches have been confirmed in our previous works by an acceptable agreement between measured and calculated plasma parameters in CF_4 + Ar [7, 12], Cl_2 + Ar [18, 19, 27] and HBr + Ar [20, 21] ICPs.

RESULTS AND DISCUSSION

Among the pure halogen-containing gases under one and the same operating conditions, the highest T_e of ~3,3 eV was measured for CF_4 plasma while the lowest T_e of ~2,4 eV is for Cl_2 plasma (Table). The reason is that the Cl_2 plasma provides the highest as well as the widest-range collisional electron energy loss compared with other two gases because the Cl_2 molecules are characterized by lowest threshold energies, ε_{th}, for both electronic excitation (ε_{th} ~ 2,5 eV) and ionization (ε_{th} ~ 11,5 eV), but by highest cross-sections for corresponding processes [22, 28, 29]. The transition to Ar-rich plasmas in all three gas systems results in monotonically increasing T_e (3,3-3,5 eV, or by 10% for CF_4 + Ar, 2,4-3,2 eV, or by 34% for Cl_2 + Ar and 2,8-3,4 eV, or by 21% for HBr + Ar at 0-80% Ar). Such situation takes place because the electronic excitation and ionization processes for Ar are characterized by higher ε_{th} values, but by lower cross-sections and corresponding rate coefficients compared with those for CF_4, Cl_2 and HBr [29, 30]. That is why, as the Ar fraction in a feed gas increases, the energy gap between the lowest excitation potentials for halogen-containing component (ε_{th} ~ 3-5 eV) and Ar atom (ε_{th} ~ 11 eV) becomes to be "transparent" for electrons. Accordingly, the dilution of CF_4, Cl_2 or HBr by argon lowers electron energy loss in inelastic collisions, increases the fraction of "fast" electrons in EEDF and shifts T_e toward higher values.

Table 1

Measured electron temperature (T_e) and ion current density (j_+) as functions of Ar fraction in CF_4 + Ar, Cl_2 + Ar and HBr + Ar gas mixtures

***Таблица 1.* Измеренные температура электронов (T_e) и плотность ионного тока (j_+) в зависимости от доли Ar в смесях CF_4 + Ar, Cl_2 + Ar и HBr + Ar**

y_{Ar}	CF_4 + Ar		Cl_2 + Ar		HBr + Ar	
	T_e, eV	j_+, mA/cm^2	T_e, eV	j_+, mA/cm^2	T_e, eV	j_+, mA/cm^2
0	3,26	1,1	2,39	1,5	2,8	1,9
0,2	3,29	1,2	2,51	1,6	2,94	2,1
0,5	3,32	1,4	2,88	1,9	3,15	2,5
0,8	3,47	2,2	3,20	3,2	3,40	3,8

Fig. 1 illustrates the influence of gas mixing ratios on the kinetics of charged species. In pure CF_4 plasma, the total ionization rate is mainly composed by R1: $CF_4 + e = CF_3^+ + F + 2e$ ($k_1 = 1{,}8{\cdot}10^{-10}$ –$2{,}6{\cdot}10^{-10}$ cm^3/s for 0-80% Ar) while the contributions of R2: $CF_3 + e = CF_3^+ + 2e$ ($k_2 = 2{,}1{\cdot}10^{-10}$–$2{,}7{\cdot}10^{-10}$ cm^3/s for 0-80% Ar) and R3: $F + e = F^+ + 2e$ ($k_3 = 8{,}3{\cdot}10^{-11}$ – $1{,}1{\cdot}10^{-10}$ cm^3/s for 0-80% Ar) do not exceed 10% and 2%, respectively. The lower rate of R2 is connected with the condition $n_{CF3} << n_{CF4}$ at $k_1 \approx k_2$, and the lowest rate of R3 results from $n_F \approx n_{CF3}$ and $k_3 << k_1$, k_2. The last condition is provided by the higher ionization threshold for F atoms (~17,4 eV) compared with CF_4 (~15,9 eV) and CF_3 (~10 eV) species. The dilution of CF_4 by An introduces the additional ionization channels, such as R4: $Ar + e = Ar^+ + 2e$ ($k_4 = 4{,}0{\cdot}10^{-10}$ – $5{,}6{\cdot}10^{-10}$ cm^3/s for 0–80% Ar) and R5: $Ar^m + e = Ar^+ + 2e$ ($k_S = 9{,}0{\cdot}10^{-8}$–$9{,}9{\cdot}10^{-8}$ cm^3/s for 0–80% Ar, where $Ar^m = Ar(^3P_0, ^3P_1, ^3P_2)$) as well as results in increasing total ionization frequency $\nu_{iz} \approx k_1 n_{CF_4} + k_4 n_{Ar} + k_5 n_{Ar^m}$ as $2{,}6{\cdot}10^4$–$1{,}1{\cdot}10^5$ s^{-1} mainly due to $k_4 > k_1$. The maximum contribution of R5 to ν_{iz} is slightly below 15% for the 20% CF_4 + 80% Ar gas mixture. This is because the condition $k_5 >> k_1$, k_4 is overcompensated by the low density of metastable Ar atoms. In pure Cl_2 plasma, the total ionization rate is composed by 74% R6: $Cl_2 + e = Cl_2^+ + 2e$ ($k_6 = 4{,}2{\cdot}10^{-10}$–$1{,}6{\cdot}10^{-9}$ cm^3/s for 0–80% Ar) and 16% R7: $Cl + e = Cl^+ + 2e$ ($k_7 = 1{,}9{\cdot}10^{-10}$–$9{,}2{\cdot}10^{-10}$ cm^3/s for 0-80% Ar). Such situation reasonably follows from $n_{Cl2} \approx n_{Cl}$ and $k_6 > k_7$. The rapid increase of T_e toward Ar-rich plasmas causes the same changes for both k_6 Cl_2 (by ~3,9 times for 0–80% Ar) and k_7 (by ~4,7 times for 0–80% Ar) and thus, results in the local increase in $k_6 n_{Cl_2} + k_7 n_{Cl}$ ($5{,}7{\cdot}10^4$–$7{,}5{\cdot}10^4$ s^{-1} for 0–50% Ar) in spite of decreasing n_{Cl_2} and n_{Cl}. Than, in the range of $y_{Ar} > >$65– 70%, the condition $k_4 n_{Ar} + k_5 n_{Ar^m} > k_6 n_{Cl_2} + k_7 n_{Cl}$

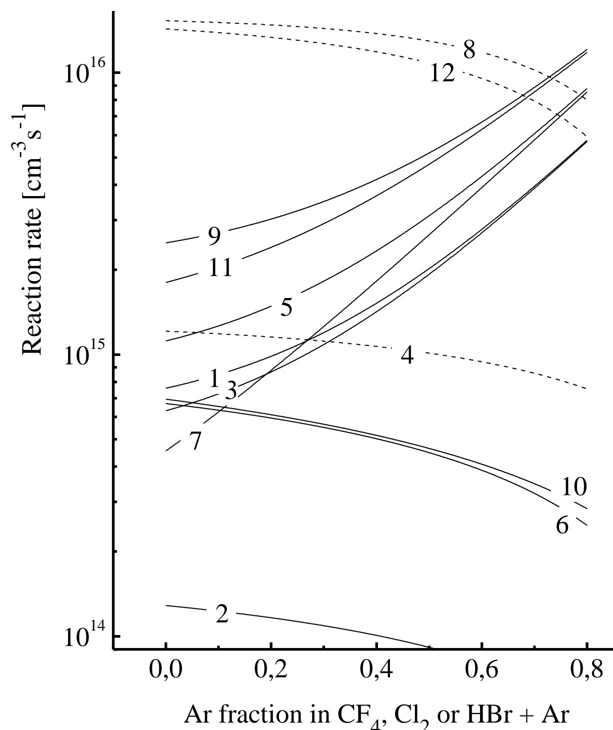

Fig. 1. Kinetics of charged (solid lines) and neutral (dashed lines) species in CF_4 + Ar (1–4), Cl_2 + Ar (5–8) and HBr + Ar (9–12) plasmas: 1, 5 and 9 – total ionization rate; 2, 6 and 10 – total attachment rate; 3, 7 and 11 – electron and ion diffusion rate; 4 – total F atom formation rate; 8 – total Cl atom formation rate; 12 – total Br atom formation rate

Рис. 1. Кинетика заряженных (сплошные линии) и нейтральных (пунктирные линии) частиц в плазме CF_4 + Ar (1 – 4), Cl_2 + Ar (5 – 8) и HBr + Ar (9 – 12): 1, 5 и 9 –суммарные скорости ионизации; 2, 6 и 10 – суммарные скорости прилипания; 3, 7 и 11 –суммарные скорости диффузионной гибели электронов и положительных ионов; 4 – суммарная скорость образования атомов F; 8 – суммарная скорость образования атомов Cl; 12 – суммарная скорость образования атомов Br

takes place. As a result, the parameter ν_{iz} increases monotonically in the range of $5{,}7{\cdot}10^4$– $9{,}9{\cdot}10^4$ s^{-1} for 0–80% Ar. In pure HBr plasma, the total ionization rate is represented by three main summands, such as R8: $HBr + e = HBr^+ + 2e$ with $k_8 = 4{,}7{\cdot}10^{-10}$ – $1{,}2{\cdot}10^{-9}$ cm^3/s for 0–80% Ar (~45%), R9: $Br_2 + e = Br_2^+ + 2e$ with $k_9 = 9{,}2{\cdot}10^{-10}$–$2{,}1{\cdot}10^{-9}$ cm^3/s for 0-80% Ar (~28%) and R10: $Br + e = Br^+ + 2e$ with $k_{10} = 4{,}8{\cdot}10^{-10}$ –$1{,}1{\cdot}10^{-9}$ cm^3/s for 0–80% Ar (~27%). The noticeable contributions from Br_2 and Br are connected with the quite high densities of these species as well as with the conditions of $k_9 > k_8$ and $k_{10} \approx k_S$. An increase in y_{Ar} results in increasing ionization rate coefficients for HBr, Br_2 and Br species, so that the parameter $k_8 n_{HBr} + k_9 n_{Br2} + k_{10} n_{Br}$ keeps the almost constant value of ~$6{,}5{\cdot}10^4$ s^{-1} up to 50% Ar. At the same time, the total effect of R4 and R5 begins to contribute the total ionization frequency from, at least, 40% Ar in the

HBr +Ar gas mixture. That is why the parameter v_{iz} increases monotonically toward Ar-rich plasmas as 6,5·10^4–1,0·10^5 s^{-1}.

From the above data, it can be understood that the total ionization frequencies in pure halogen gas plasmas are rated as v_{iz}(HBr) > v_{iz}(Cl_2) > v_{iz}(CF_4). However, the model-predicted n_e does not follow this rule (Fig. 2). The much lower frequency of the dissociative attachment for CF_4 ($k_{11}n_{CF4}$ = 4,8·10^3 s^{-1}, where R11: CF_4 + e = CF_3 + F^-) compared with Cl_2 ($k_{12}n_{Cl2}$ = 3,3·10^4 s^{-1}, where R12: Cl_2 + e = Cl + Cl^-) provides the lower decay rate for electrons and thus, results in n_e(CF_4) > n_e(Cl_2) in spite of v_{iz}(Cl_2) > v_{iz}(CF_4). At the same time, the condition $k_{12}n_{Cl2}$ > $k_{13}n_{HBr}$ + $k_{13}n_{Br2}$ = =1,9·10^4 s^{-1}, where R13: HBr + e = H + Br^- and R14: Br_2 + e = Br + Br^- does not contradict with v_{iz}(HBr) > >v_{iz}(Cl_2) and provides n_e(HBr) > n_e(Cl_2). Therefore, under one and the same operation condition, the highest n_e was found for the CF_4 plasma, and the lowest one is for the Cl_2 plasma. An increase in Ar mixing ratio results in monotonically increasing n_e in the ranges of 2,8·10^{10}–9,8·10^{10} cm^{-3} for CF_4 + Ar, 2,0·10^{10}-9,1·10^{10} cm^{-3} for Cl_2 + Ar and 3,6·10^{10}–1,2·10^{11} cm^{-3} for HBr + Ar at 0–80% Ar (Fig. 2). This effect is supported by the simultaneous increase in v_{iz} and decrease in v_{da} due to the decreasing fraction of the electronegative component in a feed gas. The densities of negative ions in pure halogen gas plasmas stand as n_{F^-} = 2,6·10^{10} cm^{-3} < n_{Cl^-} = 5,2·10^{10} cm^{-3} < <n_{Br^-} = 6,3·10^{10} cm^{-3}, as follows from the corresponding attachment rates (Fig. 1). The higher attachment rate in HBr plasma, in spite of k_{13} < k_{12}, is connected with the lower dissociation degree for HBr molecules, the noticeable (~20%) contribution from R14 and the higher electron density. The last reason lowers the n_{Br^-}/n_e ratio compared with the n_{Cl^-}/n_e, so that the highest electronegativity was found for the Cl_2 plasma. An increase in Ar mixing ratio results in monotonically decreasing attachments rates, absolute (n_{F^-} = =2,6·10^{10}-9,3·10^9, n_{Cl^-} = 5,2·10^{10}–3,0·10^{10} cm^{-3} and n_{Br^-} = 6,3·10^{10}–2,5·10^{10} cm^{-3} at 0–80% Ar) and relative (n_{F^-}/n_e = 0,96-0,13, n_{Cl^-}/n_e = 2,6–0,3 and n_{Br^-}/n_e = =1,8–0,2 at 0-80% Ar) densities of negative ions. The measured densities of positive ions in pure CF_4, Cl_2 and HBr plasmas are scaled as the corresponding ionization rates. The obtained increase in n_+ with increasing y_{Ar} (5,3·10^{10}–8,2·10^{10} cm^{-3} for CF_4 + Ar, 7,2·10^{10}–1,2·10^{11} cm^{-3} for Cl_2 + Ar and 9,9·10^{10}-1,4·10^{11} cm^{-3} for HBr + Ar at 0-80% Ar, see Fig. 2) is provided by both increasing ionization rates and decreasing decay rates of positive ions through ion-ion recombination in bulk plasma.

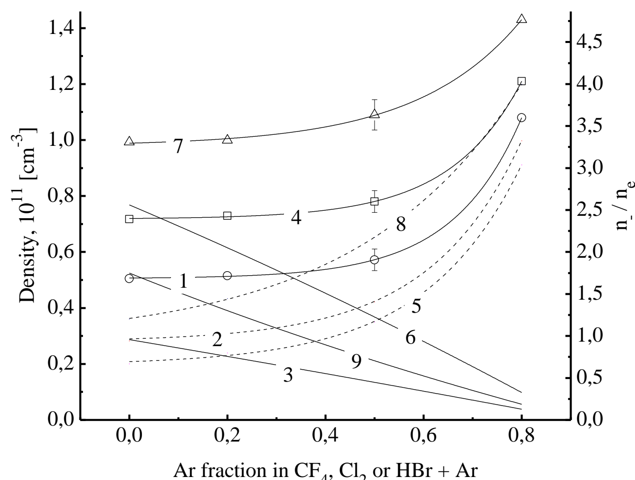

Fig. 2. Measured and model-predicted densities of charged species in CF_4 + Ar (1–3), Cl_2 + Ar (4–6) and HBr + Ar (7–9) plasmas: 1, 4 and 7 – total density of positive ions; 2, 5 and 8 – electron density; 3, 6 and 9 – relative density of negative ions

Рис. 2. Измеренные и расчетные концентрации заряженных частиц в плазме CF_4 + Ar (1 – 3), Cl_2 + Ar (4 – 6) и HBr + Ar (7 – 9): 1, 4 и 7 – суммарная концентрация положительных ионов; 2, 5 и 8 – концентрация электронов; 3, 6 и 9 –относительная концентрация отрицательных ионов

From Refs. [31-34], it can be understood that the rate of physical etching pathway, including both physical sputtering of surface atoms and ion-stimulated desorption of reaction products in ion-assisted chemical reaction, is given by $Y_S\Gamma_+$, where Γ_+ ≈ j_+/e is the total flux of positive ions on the etched surface, and Y_S is the ion-type-averaged sputtering yield. For the ion bombardment energy ε_i < 500 eV, one can assume $Y_S \sim \sqrt{M_i\varepsilon_i}$ [31, 32], where M_i is the effective ion molar mass, and ε_i depends of both negative dc bias U_{dc} and floating potential U_f as $\varepsilon_i \approx |-U_f-U_{dc}|$. Therefore, the relative change of physical etching pathway with variations of input process condition, including gas mixing ratios, can be characterized by the parameter $\sqrt{M_i\varepsilon_i}\Gamma_+$. An increase in y_{Ar} in all three gas mixtures results in decreasing $-U_{dc}$ at W_{dc} = =const (Fig. 3) and thus, in decreasing ion bombardment energy (ε_i = 395–267 eV in CF_4 + Ar, 407–288 eV in Cl_2 + Ar and 458-264 eV in HBr + Ar at 0–80% Ar). At the same time, the ion flux follows the behavior of j_+ (Table) and increases toward Ar-rich plasmas. From Fig. 3, it can be seen that, in the range of y_{Ar} < 0,5, the opposite changes of $\sqrt{M_i\varepsilon_i}$ and Γ_+ compensate one each other that results in $\sqrt{M_i\varepsilon_i}\Gamma_+$ ≈ const. However, the furthermore increase in y_{Ar} causes an increase in ion energy flux, so that the overall relative change of $\sqrt{M_i\varepsilon_i}\Gamma_+$ in the range of 0-80% Ar is by 1,7 times in CF_4 + Ar, by 1,6 times in Cl_2 + Ar and by 1,2 times in

HBr + Ar. According to the absolute values of $\sqrt{M_i \varepsilon_i}\Gamma_+$, the most advantageous conditions for the sputtering of both etched surface atoms and reaction products are in HBr + Ar plasma, and the worse conditions for the physical etching pathway are in CF_4 + Ar plasma.

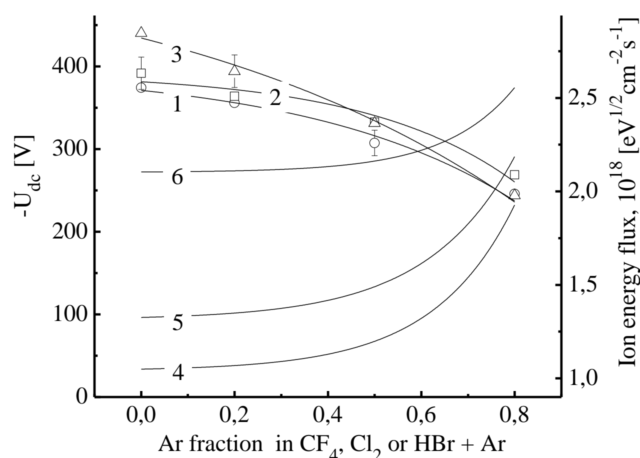

Fig. 3. Energy and particle fluxes of positive ions as functions of Ar fraction in CF_4 + Ar (1, 4), Cl_2 + Ar (2, 5) and HBr + Ar (3, 6) gas mixtures: measured negative dc bias (1 – 3) and model-predicted ion energy flux (4 – 6)

Рис. 3. Энергии и потоки положительных ионов в зависимости от доли Ar в смесях CF_4 + Ar (1, 4), Cl_2 + Ar (2, 5) и HBr + Ar (3, 6): измеренный отрицательный потенциал на подложкодержателе (1–3) и расчетные потоки энергии ионов (4 – 6)

Among the neutral species in CF_4 + Ar, Cl_2 + +Ar and HBr + Ar plasmas, the halogen atoms (F, Cl and Br) are of primary interest for the dry etching process analysis. In pure CF_4 plasma, the formation of F atoms is mainly provided by ~52% R1, ~30% R15: CF_4 + e = CF_3 + F + e (k_{15} = $1,0\cdot10^{-10}$–$1,4\cdot10^{-10}$ cm^3/s for 0–80% Ar) and ~10% R16: CF_3 + e = CF_2 + F + e (k_{16} = $6,6\cdot10^{-10}$–$7,7\cdot10^{-10}$ cm^3/s for 0-80% Ar). In pure Cl_2 plasma, the single source of Cl atoms is R17: Cl_2 + +e = 2Cl + e (k_{17} = $7,7\cdot10^{-8}$–$1,2\cdot10^{-8}$ cm^3/s for 0–80% Ar) while in pure HBr plasma the Br atoms are mainly generated through R18: HBr + e = H + Br + e (~19%), R19: Br_2 + e = 2Br + e (~55%) and R20: H + Br_2 = HBr + Br (~21%). The domination of R19 and R20 over R18 is connected with the relatively high density of Br_2 molecules which is supported by fast Br → Br_2 recombination on reactor walls as well as with k_{19} = $1,1\cdot10^{-8}$–$1,4\cdot10^{-10}$ cm^3/s >> k_{18} = $1,3\cdot10^{-9}$ – $2,1\cdot10^{-9}$ cm^3/s for 0-80% Ar. An increase in Ar fraction in a feed gas shows the similar influence on the formation kinetics of F, Cl and Br atoms and thus, on their densities in all three gas systems (Fig. 4(a)).

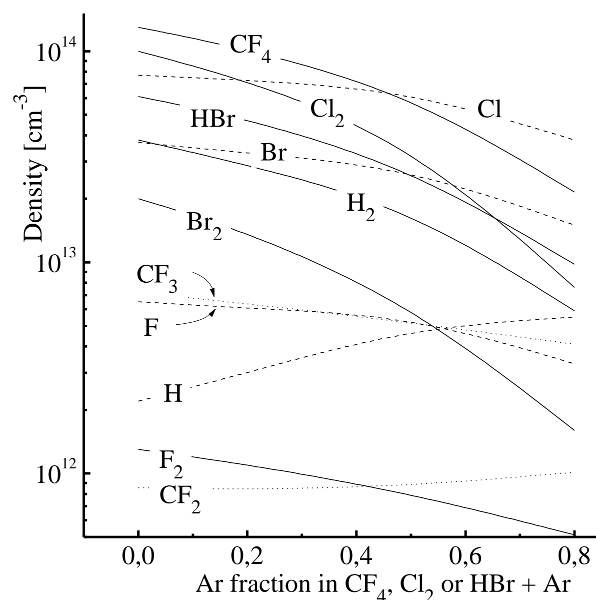

a

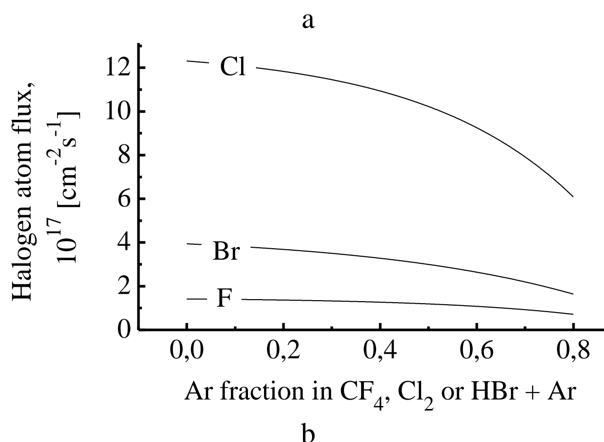

b

Fig. 4. Model-predicted densities (a) and fluxes (b) of ground-state neutral species as functions of Ar fraction in CF_4 + Ar, Cl_2 + Ar and HBr + Ar gas mixtures

Рис. 4. Расчетные концентрации (a) и потоки (b) невозбужденных нейтральных частиц в зависимости от доли Ar в смесях CF_4 + Ar, Cl_2 + Ar и HBr + Ar

The simultaneous increase in dissociation rate coefficients (due to the change of T_e) and n_e results in the noticeable increase in the frequencies of the dissociative collisions for electrons toward Ar-rich plasmas: $(k_1 + k_{15})n_e$ = 8–28 s^{-1}, $k_{17}n_e$ = 155–1000 s^{-1}, $k_{18}n_e$ = =47–252 s^{-1} and $k_{19}n_e$ = 388–1640 s^{-1} for 0-80% Ar. Though this effect is partially aligned by the decreasing fractions of the halogen-containing species in the feed gas, the formation rates and densities of F, Cl and Br atoms change non-linearly and decrease much slower than the parameter 1-y_{Ar}. As can be seen from Fig. 3, the twofold dilution of the halogen-containing component by argon (i.e. when y_{Ar} = 0,5) lowers the densities of F and Cl atoms only by 1,2 times, and the density of Br atoms by 1,5 times. Therefore, the addition of Ar leads to an increase in

electron-impact dissociation efficiencies and dissociation degrees for CF_4, Cl_2 and HBr molecules. Another remarkable issue is that, under the give set of operating conditions, the stepwise dissociations involving metastable $Ar(^3P_{0,1,2})$ species do not contribute the formation of F, Cl or Br atoms in corresponding gas systems. The reason is the low density of metastable atoms (~ $1{,}2\cdot10^{11}$ cm^{-3} in CF_4 + Ar plasma, ~ $8{,}8\cdot10^{10}$ cm^{-3} in Cl_2 + Ar plasma and ~ $1{,}0\cdot10^{11}$ cm^{-3} in HBr + Ar at 80% Ar) due to both quite low excitation rate through R21: Ar + e = Ar^m + e (ε_{th} ~ 11,6 eV) and high decay rate on reactor walls.

According to Refs. [31-33], the rate of the chemical pathway of ion-assisted chemical reaction is $\gamma_R\Gamma_X$, where $\Gamma_X \approx 0{,}25 n_X \upsilon_T$ is the flux of atomic species with the volume density of n_X, and γ_R is the probability of chemical reaction. Figure 4(b) shows that the fluxes of F, Cl and Br atoms follow the behavior of their densities in bulk plasma and keep the same quantitative ratios as was mentioned for n_F, n_{Cl} and n_{Br}. Therefore, in the case of high volatile reaction products and close reaction probabilities, the highest rate of chemical etching pathway is expected in Cl_2 + Ar plasma, and the lowest one – in the CF_4 + Ar plasma. In the case of low volatile reaction products, which can be removed from the etched surface only by the ion-stimulated desorption, γ_R depends on ion energy flux through the fraction of free surface acceptable for the adsorption of the etchant species [33, 34]. In this case, the absolute etching rates are affected by both Γ_X and $\sqrt{M_i\varepsilon_i}\Gamma_+$. Since these parameters show the opposite changes vs. y_{Ar}, one can easily expect the non-monotonic changes in the etching rates toward Ar-rich plasmas. Really, such effects have been repeatedly mentioned by experiments in CF_4 + Ar, Cl_2 + Ar and HBr + Ar plasmas [1-4].

REFERENCES

1. **Sugano T.** Applications of plasma processes to VLSI technology. New York: Wiley. 1990. 567 p.
2. **Rooth J.R.** Industrial Plasma Engineering. Philadelphia: IOP Publishing LTD. 1995. 620 p. DOI: 10.1201/9781420050868.
3. **Roosmalen A.J., Baggerman J.A.G., Brader S.J.H.** Dry etching for VLSI. New-York:Plenum Press. 1991. 490 p. DOI:10.1007/978-1-4899-2566-4.
4. **Wolf S., Tauber R.N.** Silicon Processing for the VLSI Era. V. 1. Prosess Technology. New York: Lattice Press. 2000. 416 p.
5. **Rossnagel S.M., Cuomo J.J., Westwood W.D.** Handbook of plasma processing technology. Park Ridge: Noyes Publications. 1990. 338 p.
6. **Lieberman M.A., Lichtenberg A.J.** Principles of plasma discharges and materials processing. New York: John Wiley & Sons Inc. 1994. 757 p.
7. **Efremov A. M., Kim D.-P., Kim C.-I.** Effect of gas mixing ratio on gas-phase composition and etch rate in an inductively coupled CF_4/Ar plasma. *Vacuum.* 2004. V.75. P. 133. DOI:10.1016/j.vacuum.2004.01.077.
8. **Kimura T., Noto M.** Experimental study and global model of inductively coupled CF_4/O_2 discharges. *J. Appl. Phys.* 2006. V. 100. P. 063303. DOI:10.1063/1.2345461.
9. **Kimura T., Ohe K.** Probe measurements and global model of inductively coupled Ar/CF_4 discharges. *Plasma Sources Sci. Technol.* 1999. V. 8. P. 553. DOI:10.1088/0963-0252/8/4/305.
10. **Plumb I. C., Ryan K. R.** A model of chemical processes occurring in CF_4/O_2 discharges used for plasma etching. *Plasma Chem. Plasma Proc.* 1986. V. 6. P. 205. DOI:10.1007/BF00575129.
11. **Gogolides E., Stathakopolous M., Boudouvis A.** Modelling of radio frequency plasmas in tetrafluoromethane (CF_4): the gas phase physics and the role of negative ion detachment. *J. Phys. D: Appl. Phys*. 1994. V. 27. P. 1878. DOI:10.1088/0022-3727/27/9/011.
12. **Chun I., Efremov A., Yeom G.Y., Kwon K.-H.** A comparative study of CF_4/O_2/Ar and C_4F_8/O_2/Ar plasmas for dry etching applications. *Thin Solid Films.* 2015. V. 579. P. 136. DOI:10.1016/j.tsf.2015.02.060.
13. **Ullal S.J., Godfrey A.R., Edelberg E., Braly L., Vahedy V., Aydil E.S.** Effect of chamber wall conditions on Cl and Cl_2 concentrations in an inductively coupled plasma reactor. *J. Vac. Sci. Technol.* A. 2002. V. 20. P. 43. DOI:10.1116/1.1421602.
14. **Yonemura S., Nanbu K., Sakai K.** Electron energy distributions in inductively coupled plasma: comparison of chlorine discharge with argon discharge. *Jpn. J. Appl. Phys*. 2002. V. 41. P. 6189. DOI:10.1143/JJAP.41.6189.
15. **Malyshev M.V., Donnelly V.M.** Diagnostics of chlorine inductively coupled plasmas. Measurement of electron temperatures and electron energy distribution functions. *J. Appl. Phys.* 2000. V. 87. P. 1642. DOI:10.1063/1.372072.
16. **Malyshev M.V., Fuller N.C.M., Bogart K.H.A., Donnelly V.M., Herman I.P.** Diagnostics of inductively coupled chlorine plasmas: Measurement of Cl_2^+ and Cl^+ densities. *J. Appl. Phys.* 2000. V. 88. P. 2246. DOI:10.1063/1.1288156.
17. **Efremov A.M., Kim G.-H., Kim J.-G., Kim C.-I.** Self-consistent global model for inductively coupled Cl_2 plasma: Comparison with experimental data and application for the etch process analysis. *Thin Solid Films.* 2007. V. 515. P. 5395. DOI:10.1016/j.tsf.2007.01.027.
18. **Efremov A.M., Kim G.-H., Kim J.-G., Bogomolov A.V., Kim C.-I.** Applicability of self-consistent global model for characterization of inductively coupled Cl_2 plasma. *Vacuum*. 2007. V. 81. P. 669. DOI:10.1016/j.vacuum.2006.09.017.
19. **Kwon K.-H., Efremov A., Kim M., Min N.K., Jeong J., Kim K.** Model-based analysis of plasma parameters and active species kinetics in Cl_2/X (X=Ar, He, N_2) inductively coupled plasmas. *J. Electrochem*. Soc. 2008. V. 155. P. D777. DOI:10.1149/1.2993160.
20. **Kwon K.-H., Efremov A., Kim M., Min N.K., Jeong J., Kim K.** A model-based analysis of plasma parameters and composition in HBr/X (X=Ar, He, N_2) inductively coupled plasmas. *J. Electrochem.* Soc. 2010. V. 157. P. H574. DOI:10.1149/1.3362943.

21. **Efremov A., Kim Y., Lee H.-W., Kwon K.-H.** A comparative study of HBr-Ar and HBr-Cl_2 plasma chemistries for dry etch applications. *Plasma Chem. Plasma Proc*. 2011. V. 31. P. 259. DOI:10.1007/s11090-010-9279-7.
22. **Efremov A., Kim J.H., Kwon K.-H.** A model-based comparative study of HCl and HBr plasma chemistries for dry etching purposes. *Plasma Chem. Plasma Process.* 2015. V. 35. P. 1129. DOI:10.1007/s11090-015-9639-4.
23. **Johnson E.O., Malter L**. A floating double probe method for measurements in gas discharges. *Phys. Rev*. 1950. V. 80. P. 58. DOI:10.1103/PhysRev.80.58.
24. **Sugavara M.** Plasma etching: Fundamentals and applications. New York:Oxford University Press. 1998. 469 p.
25. **Lee C., Lieberman M.A.** Global model of Ar, O_2, Cl_2, and Ar/O_2 high-density plasma discharges. *J. Vac. Sci. Technol*. A. 1995. V. 13. P. 368. DOI:10.1116/1.579366.
26. **Ashida S., Lieberman M.A.** Spatially averaged (global) model of time modulated high density chlorine plasmas. *Jpn. J. Appl. Phys.* 1997. V. 36. P. 854. DOI:10.1143/JJAP.36.854.
27. **Hsu C.-C., Nierode M.A., Coburn J.W., Graves D.B.** Comparison of model and experiment for Ar, Ar/O_2 and Ar/O_2/Cl_2 inductively coupled plasmas. *J. Phys. D: Appl. Phys.* 2006. V. 39. P. 3272. DOI:10.1088/0022-3727/39/15/009.
28. **Christophorou L.G., Olthoff J.K., Rao M.V.V.S.** Electron interactions with CF_4. *J. Phys. chem. Ref. Data* 1996. V. 25. P. 1341. DOI:10.1063/1.555986.
29. **Christophorou L.G., Olthoff J.K.** Electron interactions with Cl_2. *J. Phys. chem. Ref. Data* 1999. V. 28. P. 131. DOI:10.1063/1.556036.
30. **Peterson L.R., Allen Jr. J.E.,** Electron impact cross sections for argon. *J. Chem. Phys.* 1972. V. 56. P. 6068. DOI:10.1063/1.1677156.
31. **Jin W., Vitale S.A., Sawin H.H.** Plasma-surface kinetics and simulation of feature profile evolution in Cl_2+HBr etching of polysilicon. *J. Vac. Sci. Technol.* A. 2002. V. 20. P. 2106. DOI:10.1116/1.1517993.
32. **Gray D.C., Tepermeister I., Sawin H.H.** Phenomenological modeling of ion enhanced surface kinetics in fluorine-based plasma etching. *J. Vac. Sci. Technol*. B. 1993. V. 11. P. 1243. DOI:10.1116/1.586925.
33. **Lee C., Graves D.B., Lieberman M.A.** Role of etch products in polysilicon etching in a high-density chlorine discharge. *Plasma Chem. Plasma Process.* 1996. V. 16. P. 99. DOI:10.1007/BF01465219.
34. **Efremov A.M., Kim D. P., Kim C.-I.** Simple model for ion-assisted etching using Cl_2/Ar inductively coupled plasma: effect of gas mixing ratio. *IEEE Trans. Plasma Sci.* 2004. V. 32. P. 1344. DOI:10.1109/TPS.2004.828413.

Поступила в редакцию 30.05.2016
Принята к опубликованию 27.06.2016

Received 30.05.2016
Accepted 27.06.2016